

# Isomeric excitation of $^{229}\text{Th}$ in laser-heated clusters: Supplemental materials

Jintao Qi,<sup>1,\*</sup> Hanxu Zhang,<sup>1,\*</sup> and Xu Wang<sup>1,†</sup>

<sup>1</sup>Graduate School, China Academy of Engineering Physics, Beijing 100193, China

(Dated: February 2, 2023)

## 1. Brief theoretical framework for NEEC, NEIES, and NEET

The system under consideration consists of a nucleus, an electron, and a quantized radiation field. The total Hamiltonian can be written as

$$H = H_n + H_e + H_{\text{rad}} + H_{\text{int}} , \quad (\text{S1})$$

where  $H_n$  is the Hamiltonian for the nucleus,  $H_e$  for the electron, and  $H_{\text{rad}}$  for the radiation field.  $H_{\text{int}}$  is the interaction Hamiltonian, the form of which can be found in Ref. [S1]. The initial/final state of the system is given as a product of the state for each part

$$|i\rangle = |I_i M_i\rangle \otimes |\phi_i\rangle \otimes |0\rangle , \quad (\text{S2})$$

$$|f\rangle = |I_f M_f\rangle \otimes |\phi_f\rangle \otimes |0\rangle . \quad (\text{S3})$$

where  $|IM\rangle$  is the state of the nucleus,  $|\phi\rangle$  is the state of the electron, and  $|n\rangle$  is the number state of the radiation field.

With the help of multipole expansions, the matrix element  $\langle f|H_{\text{int}}|i\rangle$  can be derived into the following form [S1]

$$\begin{aligned} \langle f|H_{\text{int}}|i\rangle = \sum_{\lambda\mu} \frac{4\pi}{2\lambda+1} (-1)^\mu \{ \langle \phi_f | \mathcal{N}(E\lambda, \mu) | \phi_i \rangle \langle I_f M_f | \mathcal{M}(E\lambda, -\mu) | I_i M_i \rangle \\ - \langle \phi_f | \mathcal{N}(M\lambda, \mu) | \phi_i \rangle \langle I_f M_f | \mathcal{M}(M\lambda, -\mu) | I_i M_i \rangle \} , \end{aligned} \quad (\text{S4})$$

where  $\mathcal{M}(\mathcal{T}\lambda, \mu)$  and  $\mathcal{N}(\mathcal{T}\lambda, \mu)$  are the electric ( $\mathcal{T} = E$ ) or magnetic ( $\mathcal{T} = M$ ) multipole transition operators for the nucleus and for the electron, respectively.

For NEET,  $|\phi_i\rangle$  and  $|\phi_f\rangle$  are both Dirac bound states with the form

$$|\phi\rangle = |n\eta m\rangle = \begin{pmatrix} g_{n\eta}(r)\Omega_{\eta m}(\hat{r}) \\ -if_{n\eta}(r)\Omega_{-\eta m}(\hat{r}) \end{pmatrix}, \quad (\text{S5})$$

where  $n$  is the principal quantum number,  $\eta$  is a notation determined by the total angular momentum  $j$  and the orbital angular momentum  $l$ , and  $m$  is the magnetic quantum number of  $j$ .  $\Omega_{\eta m}$  are spherical spinors [S2].

For NEIES,  $|\phi_i\rangle$  and  $|\phi_f\rangle$  are both Dirac scattering states with the form [S3]

$$|\phi\rangle = |\mathbf{k}\nu\rangle^{(\pm)} = \frac{4\pi}{k} \sqrt{\frac{E + m_e c^2}{2E}} \times \sum_{\eta m} \left[ \Omega_{\eta m}^*(\hat{\mathbf{k}}) \chi^\nu \right] e^{\pm i d_{E\eta}} \begin{pmatrix} g_\eta(r) \Omega_{\eta m}(\hat{\mathbf{r}}) \\ -i f_\eta(r) \Omega_{-\eta m}(\hat{\mathbf{r}}) \end{pmatrix}, \quad (\text{S6})$$

where  $\chi_\nu$  is a spinor and  $d_{E\eta}$  is the phase shift of the partial wave.

For NEEC,  $|\phi_i\rangle$  is a Dirac scattering state and  $|\phi_f\rangle$  is a Dirac bound state.

### 1.1 NEET

The transition rate from  $|i\rangle$  to  $|f\rangle$  is

$$W_{fi} = \frac{2\pi}{\hbar} |V_{fi}|^2 \delta(E_f - E_i), \quad (\text{S7})$$

where  $V_{fi} = \langle f | H_{\text{int}} | i \rangle$ . If the system has a finite lifetime  $\tau = 1/\Gamma$ , then the  $\delta$  function will be replaced by a Lorentzian and  $W_{fi}$  becomes

$$W_{fi} = |V_{fi}|^2 \frac{\Gamma}{(E_i - E_f)^2 + \Gamma^2/4}. \quad (\text{S8})$$

Here the total decay rate  $\Gamma = \Gamma_i + \Gamma_f + \Gamma_{\text{nuc}}$ , with  $\Gamma_{i/f}$  being the spontaneous emission rate of the initial/final ionic state, and  $\Gamma_{\text{nuc}}$  being the decay rate of the nucleus [S4]. The nucleus may decay via internal conversion (IC) or  $\gamma$  radiation, so  $\Gamma_{\text{nuc}} = \Gamma_{\text{IC}} + \Gamma_\gamma$ . But since  $\Gamma_\gamma \ll \Gamma_{\text{IC}}$  for  $^{229}\text{Th}$ ,  $\Gamma_{\text{nuc}} \approx \Gamma_{\text{IC}}$ .

Introduce reduced nuclear transition probabilities

$$B(\mathcal{T}\lambda; I_i \rightarrow I_f) = \frac{1}{2I_i + 1} \sum_{M_f M_i \mu} |\langle I_f M_f | \mathcal{M}(\mathcal{T}\lambda, \mu) | I_i M_i \rangle|^2. \quad (\text{S9})$$

With Eqs. (S4), (S5) and (S9), averaging over initial states and summing over final states, the modulus square of the interaction matrix element becomes

$$|V_{fi}|^2 = 4\pi \sum_{\mathcal{T}\lambda} \left[ B(\mathcal{T}\lambda; I_i \rightarrow I_f) \frac{\kappa^{2\lambda+2}}{(2\lambda + 1)!!^2} (C_{j_i 1/2 \lambda 0}^{j_f 1/2})^2 |M_{fi}^{\mathcal{T}\lambda}|^2 \right], \quad (\text{S10})$$

where  $\kappa = \Delta E/c$  with  $\Delta E = 8.28$  eV being the energy of the isomeric state.  $C_{j_i 1/2 \lambda 0}^{j_f 1/2}$  is a Clebsch-Gordan coefficient with the relation [S5]

$$(C_{j_i 1/2 \lambda 0}^{j_f 1/2})^2 = (2l_i + 1)(2l_f + 1)(2j_f + 1) \begin{pmatrix} l_i & \lambda & l_f \\ 0 & 0 & 0 \end{pmatrix}^2 \begin{Bmatrix} l_i & \lambda & l_f \\ j_f & 1/2 & j_i \end{Bmatrix}^2. \quad (\text{S11})$$

$M_{fi}^{\mathcal{T}\lambda}$  are radial matrix elements given by

$$\begin{aligned} M_{fi}^{E\lambda} &= \int_0^\infty h_\lambda^{(1)}(\kappa r) [g_i(r)g_f(r) + f_i(r)f_f(r)] r^2 dr, \\ M_{fi}^{M\lambda} &= \frac{\eta_i + \eta_f}{\lambda} \int_0^\infty h_\lambda^{(1)}(\kappa r) [g_i(r)f_f(r) + g_f(r)f_i(r)] r^2 dr. \end{aligned} \quad (\text{S12})$$

In the above formulas  $h_\lambda^{(1)}(\kappa r)$  is the spherical Hankel function of the first kind. For  $\kappa r \ll 1$  the asymptotic form  $h_\lambda^{(1)}(\kappa r) \approx -i(2\lambda - 1)!/(\kappa r)^{\lambda+1}$  may be used [S6].

### 1.2 NEEC

The transition rate of NEEC can also be written in the form of Eq. (S8), except that  $\Gamma = \Gamma_f + \Gamma_{\text{nuc}}$  since the initial state is now a free state. The modulus square of the interaction matrix element becomes

$$|V_{fi}|^2 = 4\pi^2 \frac{E_i + m_e c^2}{E_i p_i^2} \sum_{\mathcal{T}\lambda} B(\mathcal{T}\lambda; I_i \rightarrow I_f) \frac{\kappa^{2\lambda+2}}{(2\lambda + 1)!!^2} \sum_{\eta_i} (2j_i + 1) (C_{j_i 1/2\lambda 0}^{j_f 1/2})^2 |M_{fi}^{\mathcal{T}\lambda}|^2. \quad (\text{S13})$$

The excitation cross section can be defined through  $W = \sigma j$ , with  $j$  being the flux of the initial free state

$$\begin{aligned} \sigma_{\text{NEEC}}(E_i) &= \frac{1}{j} |V_{fi}|^2 \frac{\Gamma}{(E_i - E_f)^2 + \Gamma^2/4} \\ &= \frac{4\pi^2}{c^2} \frac{E_i + m_e c^2}{p_i^3} \sum_{\mathcal{T}\lambda} [B(\mathcal{T}\lambda; I_i \rightarrow I_f) \frac{\kappa^{2\lambda+2}}{(2\lambda + 1)!!^2} \\ &\quad \times \sum_{\eta_i} (2j_i + 1) (C_{j_i 1/2\lambda 0}^{j_f 1/2})^2 |M_{fi}^{\mathcal{T}\lambda}|^2 \frac{\Gamma}{(E_i - E_f)^2 + \Gamma^2/4}]. \end{aligned} \quad (\text{S14})$$

If the electron is captured into the ground state, then  $\Gamma = \Gamma_{\text{nuc}} \approx \Gamma_{\text{IC}}$ . Otherwise  $\Gamma = \Gamma_f + \Gamma_{\text{nuc}} \approx \Gamma_f + \Gamma_{\text{IC}}$ .  $\Gamma$  is usually pretty small so the Lorentzian can still be approximated as a Dirac- $\delta$  function, which has been referred as the isolated resonance approximation [S7].

### 1.3 NEIES

Detailed discussions of NEIES have been given in Ref. [S2], and the total excitation cross section is given by

$$\begin{aligned} \sigma_{\mathcal{T}\lambda} &= \frac{8\pi^2}{c^4} \frac{p_f}{p_i} \frac{E_f + m_e c^2}{p_f^2} \frac{E_i + m_e c^2}{p_i^2} \\ &\quad \times \sum_{\mathcal{T}\lambda} [B(\mathcal{T}\lambda; I_i \rightarrow I_f) \frac{\kappa^{2\lambda+2}}{(2\lambda + 1)!!^2} \sum_{\eta_i, \eta_f} (2j_i + 1) (C_{j_i 1/2\lambda 0}^{j_f 1/2})^2 |M_{fi}^{\mathcal{T}\lambda}|^2]. \end{aligned} \quad (\text{S15})$$

## 2. Cross sections of NEEC

The cross sections of NEEC are calculated using Eq. (S14).  $\Gamma_{IC}$  is on the order of  $10^{-11}$  eV, corresponding to a lifetime on the order of  $10 \mu\text{s}$ . The spontaneous emission rates of the final atomic states  $\Gamma_f$  are obtained with the electronic wave functions calculated by the code RADIAL [S8]. The typical values of  $\Gamma_f$  are between  $10^{-8}$  and  $10^{-7}$  eV, corresponding to lifetimes on the order of 1 to 10 ns. A NEEC excitation cross section has a Lorentzian shape of width  $\Gamma$ , which is a sharp distribution approaching the Dirac- $\delta$  function.

Figure S1 shows the NEEC cross sections for the first six  $^{229}\text{Th}$  ions. For each ionic state, we calculate more than 200 NEEC channels, starting from the first bound state satisfying the NEEC condition, and then increasing the principal quantum number and angular momentum quantum number. Fig. S1 shows the largest 10 of them for each ionic state.

The highest one (of cross section about  $10^9$  barn) corresponds to electron capture into the ground state ( $7s_{1/2}$ ), which has no spontaneous emission channel. Note that although the  $7s_{1/2}$  channel has the largest cross section, it does not necessarily mean that this channel has the largest excitation efficiency. This channel is high, but it is also narrow, with a linewidth of  $8 \times 10^{-11}$  eV. After integration over energy, the  $7s_{1/2}$  channel may not be the dominant one.

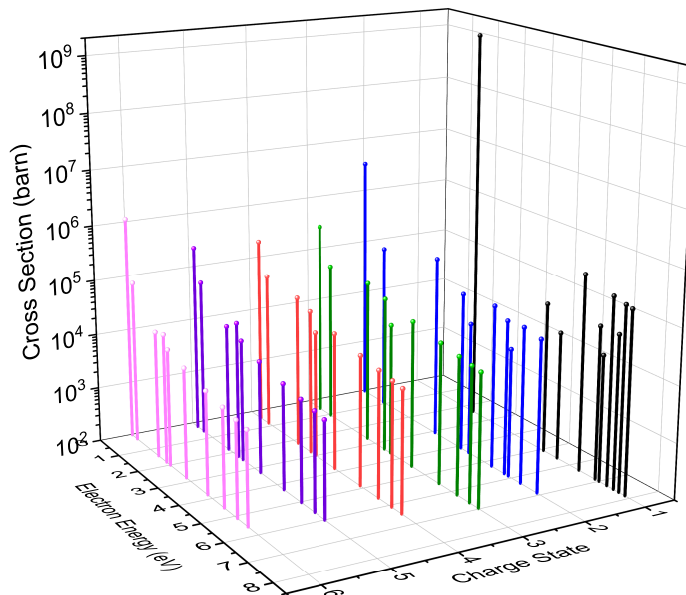


FIG. S1: Isomeric excitation cross sections of  $^{229}\text{Th}^{1+,2+,3+,4+,5+,6+}$  ions through NEEC processes. For each ionic state, the largest 10 NEEC channels are shown.

### 3. Calculation benchmarks

We have checked our calculations and compared them with available results in the literature.

(1) The most direct comparison can be made to the decay half-life of neutral  $^{229}\text{Th}$  via internal conversion. The experimental value is reported to be  $7 \pm 1 \mu\text{s}$  [S9]. Our calculation gives the half-life to be  $5.7 \mu\text{s}$ , using the reduced transition probabilities  $B(M1)_{\downarrow} = 0.0076$  W.u. and  $B(E2)_{\downarrow} = 27$  W.u. as given by Minkov and Pálffy [S10]. There are some degrees of uncertainty with these values. For example, the same authors later update them to a range of values with  $B(M1)_{\downarrow}$  between 0.005 and 0.008 W.u. and  $B(E2)_{\downarrow}$  between 30 and 50 W.u. [S11]. Using this range, our calculation gives the half-life in the range between 5.4 and  $8.7 \mu\text{s}$ , which covers the experimental values. In fact, *the accuracy of our results is mostly limited by the knowledge of the nuclear transition probabilities, instead of by the electronic calculations.* The nuclear transition probabilities are roughly uncertain by a factor of two, as given above. This is the current status of human knowledge. This uncertainty affects the absolute value of NEEC and NEIES, but it will not affect the relative ratio between them.

(2) Our calculations of the NEIES cross section of  $^{229}\text{Th}$  [S2] agree almost exactly with the results of Tkalya [S12] who uses a density functional theory to describe the many-electron interactions.

(3) Tkalya also calculated the internal conversion coefficient (ICC) of  $^{229}\text{Th}$  [S13]. He considered the  $^{229}\text{Th}^{4+}$  ion and calculated the ICC when putting an electron in the Rydberg  $n(s1/2)$  state. He uses the density functional theory for the electronic part. The ICC as a function of the main quantum number  $n$  is shown in Fig. S2. We did the same calculation using RADIAL and our results agree very closely to Tkalya's.

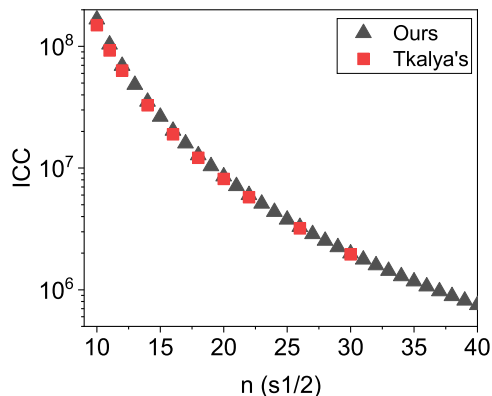


FIG. S2: Comparison of calculation results on ICC for the Rydberg  $n(s1/2)$  states of the  $^{229}\text{Th}^{4+}$  ion.

(4) For other nuclei, our NEEC results using RADIAL agree within a few percent to results given by the GRASP92 package [S14]. For example, the following Table S1 compares the resonant strengths of NEEC of  $^{57}\text{Fe}$  and  $^{157}\text{Gd}$  using GRASP92 and RADIAL.  $E_n$  is the nuclear excitation energy,  $nlj$  is the orbital into which the electron recombines, and  $S$  is the resonant strength (i.e. energy integrated NEEC cross section).

TABLE S1: NEEC resonant strengths calculated by GRASP92 and RADIAL.

			GRASP92	RADIAL
Element	$E_n$ (keV)	$nlj$	$S$ (b eV)	$S$ (b eV)
$^{57}_{26}\text{Fe}$	14.412	1s1/2	$1.19 \times 10^{-3}$	$1.13 \times 10^{-3}$
$^{157}_{64}\text{Gd}$	54.533	2s1/2	$2.86 \times 10^{-2}$	$2.99 \times 10^{-2}$
		2p1/2	$4.07 \times 10^{-3}$	$4.26 \times 10^{-3}$
		2p3/2	$7.12 \times 10^{-4}$	$7.46 \times 10^{-4}$

#### 4. Nuclear excitation rates via NEET

NEET occurs when the energy difference between two electronic bound states matches the nuclear isomeric energy  $\Delta E = 8.28$  eV. In the main text, we show that if we want to isolate the NEEC mechanism, the intensity of the laser pulse should be lower than about  $10^{14}$  W/cm<sup>2</sup>, with which the contribution from NEIES can be neglected. Here we present results for NEET and show that the rate of NEET at this intensity is negligible compared to that of NEEC or NEIES.

With  $10^{14}$  W/cm<sup>2</sup> the dominant ions are  $^{229}\text{Th}^{2+}$  and  $^{229}\text{Th}^{3+}$ . We calculate NEET for  $^{229}\text{Th}^+$ ,  $^{229}\text{Th}^{2+}$  and  $^{229}\text{Th}^{3+}$ . The energy levels and wave functions of the ionic states are calculated with the RADIAL code [S8], which uses a Dirac-Hartree-Fock-Slater method. We try to find  $\phi_i$ - $\phi_f$  pairs that satisfy: (1) the energy constraint  $|E_i - E_f - 8.28| < 0.1$  eV, and (2) the angular-momentum constraint that this channel can excite the nucleus through  $M1$  or  $E2$  transitions.

For the  $^{229}\text{Th}^+$  ion, a single transition  $7p_{3/2} \rightarrow 5f_{5/2}$  is found satisfying both constraints ( $|E_i - E_f - 8.28| = 0.03$  eV,  $M1$  and  $E2$  transitions). Using Eq. (S10)

$$|V_{fi}|^2(7p_{3/2} \rightarrow 5f_{5/2}) = 1.53 \times 10^{-20} \text{ a.u.} \quad (\text{S16})$$

The initial electronic state  $7p_{3/2}$  can decay via spontaneous emission, the rate of which is calculated to be  $\Gamma_i = 3.76 \times 10^{-9}$  a.u. using the wave functions of the relevant electronic states. This rate corresponds to a lifetime of 6.4 ns. The final state  $5f_{5/2}$  does not have a spontaneous emission channel. For the nuclear part, the IC channel is closed because the energy of the final electronic state  $5f_{5/2}$  is below  $-8.28$  eV. The  $\gamma$  decay rate  $\Gamma_\gamma (= 1.28 \times 10^{-20}$  a.u.) is negligible due to the very long lifetime ( $T_{1/2} \approx 1880$  s) [S15]. Therefore the total decay rate for this NEET channel  $\Gamma \approx \Gamma_i = 3.76 \times 10^{-9}$  a.u., and the rate of NEET is calculated to be

$$W(7p_{3/2} \rightarrow 5f_{5/2}) = 2.02 \times 10^{-6} \text{ s}^{-1}. \quad (\text{S17})$$

This value is the rate of NEET for a single  $^{229}\text{Th}^+$  ion assuming that the ion is prepared in the  $7p_{3/2}$  initial state. If we use this rate, we find that during the cluster lifetime of 1 ps, the probability of nuclear excitation for a single nucleus is about  $2 \times 10^{-18}$ , which is 11 orders of magnitude smaller than the NEEC probability on the order of  $10^{-7}$ .

Similar calculations can be performed for the  $^{229}\text{Th}^{2+}$  ion and  $^{229}\text{Th}^{3+}$  ion. For the  $^{229}\text{Th}^{2+}$  ion, four NEET channels are found satisfying the above two constraints, as listed in Table S2. These four channels yield a total rate of about  $2.44 \text{ s}^{-1}$ . The excitation probability during the lifetime of the cluster is about  $2.44 \times 10^{-12}$  per nucleus, which is about 5 orders of magnitude smaller than the NEEC probability.

TABLE S2: NEET channels in  $^{229}\text{Th}^{2+}$ 

$\phi_i$	$\phi_f$	type	$ E_i - E_f - 8.28 $ (eV)	$ V_{fi} ^2$ (a.u.)	$\Gamma_i$ (a.u.)	$\Gamma_f$ (a.u.)	$W_{\text{NEET}}$ ( $\text{s}^{-1}$ )
$9p_{3/2}$	$7p_{3/2}$	M1,E2	0.025	$6.78 \times 10^{-16}$	$4.32 \times 10^{-9}$	$2.09 \times 10^{-8}$	0.87
$15d_{3/2}$	$8s_{1/2}$	M1,E2	0.012	$4.14 \times 10^{-19}$	$8.22 \times 10^{-10}$	$1.41 \times 10^{-8}$	$1.3 \times 10^{-3}$
$15d_{5/2}$	$8s_{1/2}$	E2	0.0076	$6.92 \times 10^{-22}$	$5.60 \times 10^{-10}$	$1.41 \times 10^{-8}$	$5.42 \times 10^{-6}$
$16s_{1/2}$	$8s_{1/2}$	M1	0.032	$3.39 \times 10^{-15}$	$1.27 \times 10^{-9}$	$1.41 \times 10^{-8}$	1.57

TABLE S3: NEET channels in  $^{229}\text{Th}^{3+}$ 

$\phi_i$	$\phi_f$	type	$ E_i - E_f - 8.28 $ (eV)	$ V_{fi} ^2$ (a.u.)	$\Gamma_i$ (a.u.)	$\Gamma_f$ (a.u.)	$W_{\text{NEET}}$ ( $\text{s}^{-1}$ )
$12p_{3/2}$	$8p_{3/2}$	M1,E2	0.055	$1.70 \times 10^{-16}$	$2.61 \times 10^{-9}$	$1.85 \times 10^{-8}$	0.037
$24s_{1/2}$	$9s_{1/2}$	M1	0.037	$8.15 \times 10^{-16}$	$7.49 \times 10^{-10}$	$3.21 \times 10^{-8}$	0.604
$25s_{1/2}$	$9s_{1/2}$	M1	0.014	$7.04 \times 10^{-16}$	$6.48 \times 10^{-10}$	$3.21 \times 10^{-8}$	0.075
$24d_{3/2}$	$9s_{1/2}$	M1,E2	0.016	$8.95 \times 10^{-20}$	$3.06 \times 10^{-10}$	$3.21 \times 10^{-8}$	$3.39 \times 10^{-6}$
$26s_{1/2}$	$8d_{3/2}$	M1,E2	0.006	$1.59 \times 10^{-19}$	$5.65 \times 10^{-10}$	$1.95 \times 10^{-8}$	$2.68 \times 10^{-3}$
$25d_{3/2}$	$8d_{3/2}$	M1,E2	0.004	$4.17 \times 10^{-19}$	$2.67 \times 10^{-10}$	$1.95 \times 10^{-8}$	$1.91 \times 10^{-4}$
$25d_{5/2}$	$8d_{3/2}$	M1,E2	0.003	$6.77 \times 10^{-20}$	$1.59 \times 10^{-10}$	$1.95 \times 10^{-8}$	$3.69 \times 10^{-5}$

For the  $^{229}\text{Th}^{3+}$  ion, more than 20 NEET channels are found satisfying the above two constraints. Table S3 lists seven channels with the largest NEET rates. These seven channels yield a total rate of about  $0.72 \text{ s}^{-1}$ . The excitation probability during the lifetime of the cluster is about  $7.2 \times 10^{-13}$  per nucleus, which is about 6 orders of magnitude smaller than the NEEC probability.

There is another big difference between NEET and NEEC/NEIES. In the cluster, or a plasma environment in general, NEEC and NEIES happen to each ion. But NEET only happens to a small fraction of ions excited to the desired electronic states ( $\phi_i$ 's here). In thermal equilibrium this fraction can be estimated using the Boltzmann distribution function. This condition further reduces the importance of NEET.

From the above calculations, we can conclude that nuclear excitation through NEET can be safely neglected compared to NEEC or NEIES, for laser intensities around or below  $10^{14} \text{ W/cm}^2$ .

## 5. Ion charge distributions

The ion charge distribution is determined by the laser intensity. For example, Fig. S3 shows the ionization probabilities of the Th atom under four different laser peak intensities, calculated using the Ammosov-Delone-Krainov tunnel-ionization formula [S16]. For intensity  $10^{14}$  W/cm<sup>2</sup>, the first two electrons are completely emitted and the third electron is emitted with a probability of about 30%. The emission of the fourth electron is negligible. This means that under this intensity, 70% of the ions are Th<sup>2+</sup> and 30% are Th<sup>3+</sup>. For intensity  $2 \times 10^{14}$  W/cm<sup>2</sup>, the emission probability of the third electron increases to about 90% while the emission of the fourth electron is still negligible. So under this intensity, 90% of the ions are Th<sup>3+</sup> and 10% are Th<sup>2+</sup>. For intensity  $10^{15}$  W/cm<sup>2</sup>, the first three electrons are completely emitted and the fourth electron is emitted with a probability of about 95%. The emission of the fifth electron is negligible. This means that under this intensity, 95% of the ions are Th<sup>4+</sup> and 5% are Th<sup>3+</sup>. For intensity  $2 \times 10^{15}$  W/cm<sup>2</sup>, the emission of the fourth electron is complete while the emission of the fifth electron is still negligible. So under this intensity, all ions are Th<sup>4+</sup>.

One can see from the above examples that given a laser intensity, the ion charge distribution is quite narrow: there are usually only one or two charge states.

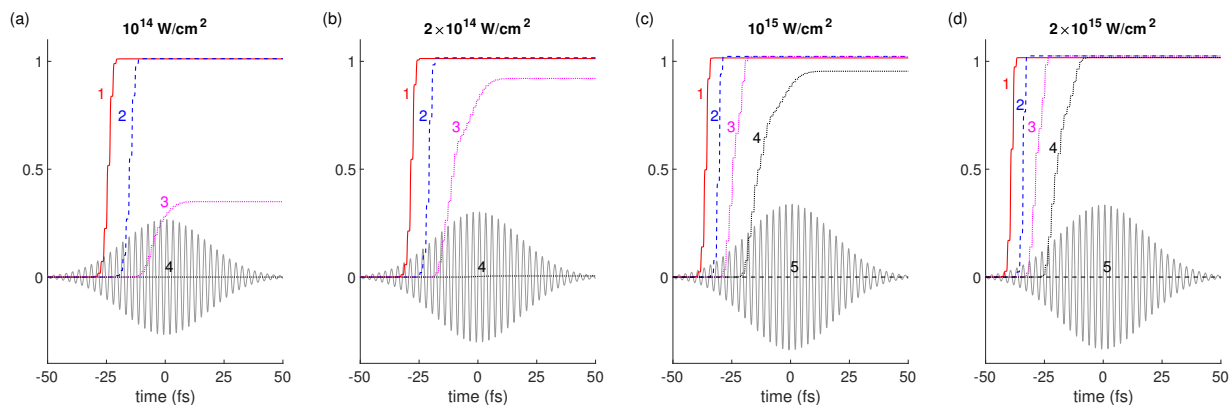


FIG. S3: Ionization probability of the Th atom during the laser pulse under four different laser peak intensities, as labeled on top of each figure. The first-emitted (second-emitted, ...) electron is labeled by number “1” (“2”, ...). The gray curve illustrates the laser pulse (the laser electric field). The laser wavelength is 800 nm and the pulse duration is 30 fs (FWHM in intensity).

## 6. Photoexcitation processes

The following three photoexcitation processes exist in laser-heated clusters: (1) Direct excitation by the femtosecond laser pulse; (2) Photoexcitation by blackbody radiations; (3) Photoexcitation by bremsstrahlung. Results show that photoexcitation of nuclei is negligible compared to NEEC or NEIES.

### 6.1 Direct laser excitation

Nuclear excitation by the femtosecond laser pulse that heats the cluster can be calculated from first-order perturbation theory. The nucleus is initially in the ground state  $|i\rangle = |I_i M_i\rangle$ , and the probability amplitude for the nucleus in the isomeric state  $|f\rangle = |I_f M_f\rangle$  is

$$b_{if}(t) = -\frac{i}{\hbar} \int_0^t \langle I_f M_f | H_{\text{int}}(t') | I_i M_i \rangle e^{i\omega_0 t'} dt', \quad (\text{S18})$$

where  $\omega_0 = \Delta E/\hbar$  is the transition frequency of the isomeric state. Averaging over initial states and summing over final states, the probability of direct laser excitation is then

$$P_{if}(t) = \frac{1}{2I_i + 1} \sum_{M_i M_f} |b_{if}(t)|^2. \quad (\text{S19})$$

The interaction Hamiltonian is written as  $H_{\text{int}}(t) = c^{-1} \int d\tau \mathbf{j}_n(\mathbf{r}) \cdot \mathbf{A}(\mathbf{r}, t)$ , where  $\mathbf{j}_n$  is the nuclear charge current and  $\mathbf{A}(\mathbf{r}, t)$  is the vector potential of the laser field. With the help of electric and magnetic multipole fields, one can express the interaction Hamiltonian consisting of electric and magnetic components as shown in Ref. [S17]. For the magnetic transitions, the matrix element is

$$\langle I_f M_f | H_{\text{int}}(t) | I_i M_i \rangle = A(t) \sqrt{2\pi} \sqrt{\frac{\lambda + 1}{\lambda}} \frac{k^\lambda}{(2\lambda + 1)!!} C_{I_i - M_i \lambda - \sigma}^{I_f M_f} \sqrt{2I_i + 1} \sqrt{B(M\lambda; I_i \rightarrow I_f)}, \quad (\text{S20})$$

where  $A(t)$  denotes the time-dependent amplitude of the vector potential,  $k$  is the wave vector, and  $\sigma$  is the polarization. Similarly, the matrix element for the electric transitions is

$$\langle I_f M_f | H_{\text{int}}(t) | I_i M_i \rangle = A(t) \sqrt{2\pi} \sqrt{\frac{(2\lambda + 1)(\lambda + 1)}{\lambda}} \frac{k^\lambda}{(2\lambda + 1)!!} C_{I_i - M_i \lambda - \sigma}^{I_f M_f} \sqrt{2I_i + 1} \sqrt{B(E\lambda; I_i \rightarrow I_f)}. \quad (\text{S21})$$

In this work, the laser pulse is linearly polarized with wavelength 800 nm. The laser electric field is assumed to have a Gaussian temporal envelope of duration 30 fs (FWHM in intensity). For peak intensity  $I = 10^{14}$  W/cm<sup>2</sup>, the calculated photoexcitation probability is shown in Fig. S4. One can see that the excitation probability is on the order of  $10^{-14}$  for a single nucleus during the laser

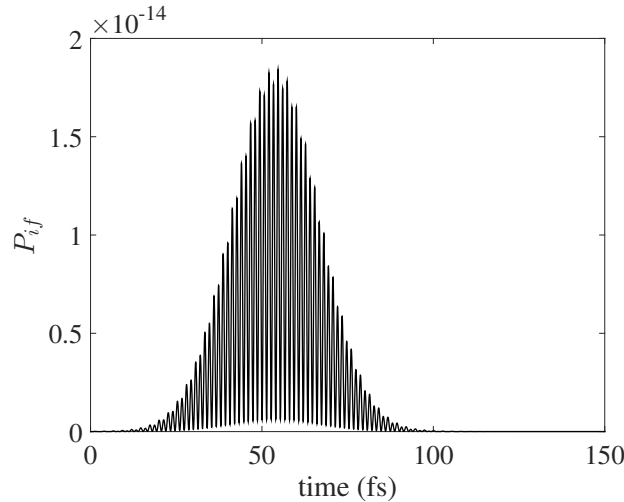


FIG. S4: Photoexcitation probability of a single  $^{229}\text{Th}$  nucleus by the fs laser pulse that heats the cluster. The laser has wavelength 800 nm, duration 30 fs (FWHM in intensity), and peak intensity  $10^{14}$  W/cm $^2$ .

pulse. This probability is negligible compared to the excitation probabilities induced by NEEC or NEIES (on the order of  $10^{-7}$ ). Besides, when the laser pulse is over, the population of the nucleus mostly goes back to the ground state. Therefore we can conclude that direct photoexcitation by the femtosecond laser pulse can be neglected.

## 6.2 Photoexcitation by blackbody radiations and by bremsstrahlung

In a laser-heated cluster, photons are present as blackbody radiations and bremsstrahlung, both of which have broad spectra. The nuclei can be excited by absorption of photons resonant with the isomeric state. The photoexcitation rate is calculated as

$$W_\gamma = \int \sigma_\gamma^{i \rightarrow f}(\varepsilon) \phi_\gamma(\varepsilon, T_e) d\varepsilon, \quad (\text{S22})$$

where the nuclear photoexcitation cross section  $\sigma_\gamma^{i \rightarrow f}(\varepsilon) = \frac{2\pi^2}{k^2} \frac{2I_f + 1}{2I_i + 1} \Gamma_\gamma^{f \rightarrow i} L_d(\varepsilon - \Delta E)$ , with  $\Gamma_\gamma^{f \rightarrow i}$  being the radiative decay rate of the isomeric state [S18], and  $L_d$  being a Lorentzian function for the mismatch between the photon energy  $\varepsilon$  and the isomeric energy  $\Delta E$ .  $\phi_\gamma$  is the photon flux.

Blackbody photons obey Planck's law, and the photon flux is given as

$$\phi_\gamma^{\text{blackbody}}(\varepsilon, T_e) d\varepsilon = c N_\gamma^{\text{Planck}}(\varepsilon, T_e) d\varepsilon = \frac{\varepsilon^2 d\varepsilon}{\pi^2 c^2 \hbar^3 [e^{\varepsilon/T_e} - 1]}, \quad (\text{S23})$$

then the photoexcitation rate induced by blackbody radiations is

$$W_\gamma^{\text{blackbody}} = \frac{2\pi^2}{k^2} \frac{2I_f + 1}{2I_i + 1} \Gamma_\gamma^{f \rightarrow i} \phi_\gamma^{\text{blackbody}}(\Delta E, T_e). \quad (\text{S24})$$

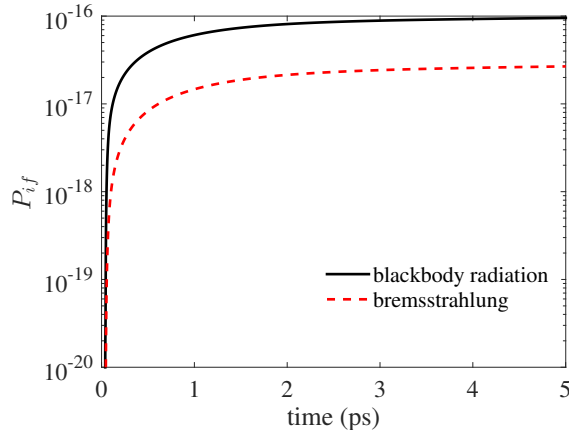


FIG. S5: Photoexcitation probabilities of a single  $^{229}\text{Th}$  nucleus via blackbody radiations and bremsstrahlung.

For the case of bremsstrahlung, the photon flux is defined similarly to Ref. [S19]

$$\phi_{\gamma}^{\text{bremsstrahlung}}(\varepsilon, T_e, n_e)d\varepsilon = \int_{E_e} \frac{d\sigma_{\text{bremsstrahlung}}}{d\varepsilon} \phi_e(E_e, T_e, n_e)dE_e d\varepsilon, \quad (\text{S25})$$

where  $d\sigma_{\text{bremsstrahlung}}/d\varepsilon$  is the bremsstrahlung differential cross section in photon energy, for which we adopt formula 3CS(a) of Ref. [S20].  $\phi_e(E_e, T_e, n_e)dE_e = n_e f(E_e)v_e(E_e)dE_e$  is the electron flux. The photoexcitation rate induced by bremsstrahlung

$$W_{\gamma}^{\text{bremsstrahlung}} = \frac{2\pi^2}{k^2} \frac{2I_f + 1}{2I_i + 1} \Gamma_{\gamma}^{f \rightarrow i} \phi_{\gamma}^{\text{bremsstrahlung}}(\Delta E, T_e, n_e). \quad (\text{S26})$$

In a laser-heated cluster, the temperature drops during cluster expansion which leads to a time-dependent nuclear photoexcitation rate via blackbody radiations or bremsstrahlung. The photoexcitation probabilities for a single  $^{229}\text{Th}$  nucleus can be calculated with  $P_{if}(t) = \int_0^t W_{\gamma}(t')dt'$ . Fig. S5 shows  $P_{if}(t)$  by blackbody radiations and bremsstrahlung, after being heated by a laser pulse of peak intensity  $I = 10^{14} \text{ W/cm}^2$ . The photoexcitation probabilities via blackbody radiations and bremsstrahlung are between  $10^{-17}$  and  $10^{-16}$ , which are about 10 orders of magnitude smaller than those induced by NEEC or NEIES.

### 7. Effect of plasma-induced energy-level shifts

In a plasma environment, the energy levels of an ion are shifted due to charge screening, leading to effects like ionization potential depression. Here we estimate the effect of this energy-level shift on NEEC.

The nano-plasma environment of a laser-heated cluster is in the so-called ion-sphere regime (in contrast to the low-ion-density Debye-shielding regime), and it can be well described by the ion-sphere model [S21]. Without going into the detailed derivations, we just cite the result that we need here: From the ion-sphere model, a bound ionic state is shifted in energy by a ratio of [S22]

$$\frac{a_0}{Z} \left( \frac{4\pi n}{3} \right)^{1/3}, \quad (\text{S27})$$

where  $a_0$  is the Bohr radius,  $Z$  is the ion charge, and  $n$  is the ion density. Using the cluster density of  $3 \times 10^{22} \text{ cm}^{-3}$ , we get a ratio of 13% for  $\text{Th}^{2+}$  and 8.8% for  $\text{Th}^{3+}$ , which are two relevant ions for laser intensities around  $10^{14} \text{ W/cm}^2$ . So the energy shifts of NEEC channels are below 1 eV due to the low resonant energy of 8.28 eV.

The leading effect of this energy-level shift on NEEC is that a (slightly) higher continuum state is needed to fulfill the resonant condition [S19]. One can estimate this effect by updating the continuum wave function while keeping the bound-state wave function unchanged in the NEEC matrix element [Eqs. (S12, S13)]. The final result is shown in Fig. S6 for laser intensity  $10^{14} \text{ W/cm}^2$ . The NEEC yield is found to be decreased by about 12%, which is nevertheless within the expected accuracy of our calculations.

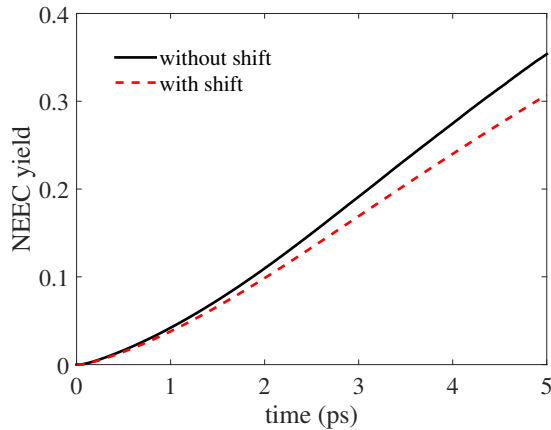


FIG. S6: Production yield of  $^{229m}\text{Th}$  per cluster via NEEC with or without the effect of plasma-induced energy-level shifts. The laser intensity is  $10^{14} \text{ W/cm}^2$ .

---

\* These two authors contributed equally

† Corresponding author: xwang@giscaep.ac.cn

- [S1] K. Alder, A. Bohr, T. Huus, B. Mottelson, and A. Winther, *Rev. Mod. Phys.* **28**, 432 (1956).
- [S2] H. Zhang, W. Wang, and X. Wang, *Phys. Rev. C* **106**, 044604 (2022).
- [S3] V. B. Berestetskii, E. M. Lifshitz, and L. P. Pitaevskii, *Quantum Electrodynamics* (Butterworth-Heinemann, 1982), Vol. 4.
- [S4] E. V. Tkalya, *Nucl. Phys. A.* **539**, 209 (1992).
- [S5] A. Bohr and B. R. Mottelson, *Nuclear Structure. Vol. I: Single-Particle Motion* (World Scientific, London, 1998).
- [S6] M. Abramowitz, I. A. Stegun, and R. H. Romer, *Handbook of mathematical functions with formulas, graphs, and mathematical tables* (National Bureau of Standards, Washington, D.C., 1964).
- [S7] A. Pálffy, W. Scheid and Z. Harman, *Phys. Rev. A.* **73**, 012715 (2006).
- [S8] F. Salvat and J. M. Fernandez-Varea, *Comput. Phys. Commun.* **240**, 165 (2019).
- [S9] B. Seiferle, et al., *Phys. Rev. Lett.* **118**, 042501 (2017).
- [S10] N. Minkov and A. Pálffy, *Phys. Rev. Lett.* **118**, 212501 (2017).
- [S11] N. Minkov and A. Pálffy, *Phys. Rev. C* **103**, 014313 (2021).
- [S12] E. V. Tkalya, *Phys. Rev. Lett.* **124**, 242501 (2020).
- [S13] E. V. Tkalya, *Phys. Rev. C* **100**, 054316 (2019).
- [S14] A. Pálffy, Doctor Thesis, Justus-Liebig-University Giessen (2006).
- [S15] P. V. Borisjuk, E. V. Chubunova, N. N. Kolachevsky, Yu. Yu. Lebedinskii, O. S. Vasiliev and E. V. Tkalya, arXiv:1804.00299 (2018).
- [S16] M. V. Ammosov, N. B. Delone, and V. P. Krainov, *Sov. Phys. JETP* **64**, 1191 (1986).
- [S17] A. Pálffy, J. Evers, and C. H. Keitel, *Phys. Rev. C* **77**, 044602 (2008).
- [S18] P. Ring and P. Schuck, *The Nuclear Many-Body Problem* (Springer, New York, 1980).
- [S19] J. Gunst, Y. Wu, C. H. Keitel, and A. Pálffy, *Phys. Rev. E* **97**, 063205 (2018).
- [S20] H. W. Koch and J. Motz, *Rev. Mod. Phys.* **31**, 920 (1959).
- [S21] H. R. Griem, *Principles of Plasma Spectroscopy* (Cambridge University Press, Cambridge, 1997).
- [S22] R. P. Drake, *High-Energy-Density Physics* (Springer, Berlin, 2010).